International Journal of Information, Control and Computer Sciences
ISSN: 2517-9942
Vol:3, No:12, 2009

Adaptive Fuzzy Control of Stewart Platform under Actuator Saturation

Dongsu Wu, Hongbin Gu and Peng Li

Abstract**—**A novel adaptive fuzzy trajectory tracking algorithm of Stewart platform based motion platform is proposed to compensate path deviation and degradation of controller's performance due to actuator torque limit. The algorithm can be divided into two parts: the real-time trajectory shaping part and the joint space adaptive fuzzy controller part. For a reference trajectory in task space whenever any of the actuators is saturated, the desired acceleration of the reference trajectory is modified on-line by using dynamic model of motion platform. Meanwhile an additional action with respect to the difference between the nominal and modified trajectories is utilized in the non-saturated region of actuators to reduce the path error. Using modified trajectory as input, the joint space controller incorporates compute torque controller, leg velocity observer and fuzzy disturbance observer with saturation compensation. It can ensure stability and tracking performance of controller in present of external disturbance and position only measurement. Simulation results verify the effectiveness of proposed control scheme.

Keywords**—** Actuator saturation; adaptive fuzzy control; Stewart platform; trajectory shaping; flight simulator.

I. INTRODUCTION

STEWART platform has been widely used in flight simulator, driving simulator, parallel machine tools and etc. Although it has many advantages over conventional serial mechanism including high structural stiffness, heavy load capacity and possibility of lightweight design, it may encounter problems such as limited workspace, singularity problem and difficulty to exploit the dynamic potential due to complexity of transformation equations between joint space and operational space [1].

In order to achieve high performance for Stewart platform, both effective trajectory planning method and robust controller should be carefully designed considering capability of actuators and external disturbances. The early research of actuator saturation problem in control system limited in linear systems [2] and gradually extended to nonlinear systems such as flight control systems [3] and serial manipulators [4]. But for Stewart platform, fewer results have been reported in public. The controller design methods considering actuator saturation can be mainly divided into two kinds: (1) Consider actuator saturation during controller design phase, including anti-windup [5], robust control [4], model predictive control [6] and so on. These methods are most suitable for linear system. (2) Trajectory modification. This kind of methods can modify reference trajectory if trajectory varies too fast, which ensures the actuators unsaturated. But it can not ensure the performance of controller when large external disturbances are existed.

This paper proposes an adaptive fuzzy controller and real-time trajectory shaping scheme for Stewart platform under actuator saturation. The real-time trajectory shaping algorithm makes use of dynamic model information to predict saturation condition and thus modifies the reference trajectory. The adaptive fuzzy controller incorporates computing torque controller, link velocity observer and fuzzy disturbance observer with the saturation compensation. It can ensure stability and tracking performances of the controller in present of external disturbance and position only measurement.

Dongsu Wu is with College of Civil Aviation, Nanjing University of Aeronautics and Astronautics, 210016, China (e-mail: tissle@nuaa.edu.cn)
Hongbin Gu is with College of Civil Aviation, Nanjing University of Aeronautics and Astronautics, 210016, China.
Peng Li is with College of Civil Aviation, Nanjing University of Aeronautics and Astronautics, 210016, China

II. DYNAMIC MODEL OF STEWART PLATFORM

An operational space dynamic model of the Stewart platform is derived by means of Newton-Euler method as follows,

$$\boldsymbol{M}(\boldsymbol{X})\ddot{\boldsymbol{X}} + \boldsymbol{H}(\boldsymbol{X},\dot{\boldsymbol{X}}) = \boldsymbol{J}^T\boldsymbol{F} + \boldsymbol{D}\,, \tag{1}$$

where $\boldsymbol{X}, \dot{\boldsymbol{X}}, \ddot{\boldsymbol{X}}$ separately correspond to position, velocity and acceleration information of a payload platform in operational-space; $\boldsymbol{M}(\boldsymbol{X})$ is the inertia matrix; $\boldsymbol{H}(\boldsymbol{X},\dot{\boldsymbol{X}})$ the nonlinearity including Coriolis, centrifugal and gravity force; $\boldsymbol{F}$ the driving force of actuators; $\boldsymbol{J}$ the Jacobian matrix and $\boldsymbol{D}$ the external disturbance.

The joint-space dynamic model needs transformation between joint space and operational space, which is related to inverse acceleration kinematic analysis of the Stewart platform,

$$\ddot{\boldsymbol{L}} = \boldsymbol{J}\ddot{\boldsymbol{X}} + \dot{\boldsymbol{J}}\dot{\boldsymbol{X}}\,, \tag{2}$$

where $\ddot{\boldsymbol{L}}$ corresponds to acceleration of links, $\dot{\boldsymbol{J}}$ is the differentiation of Jacobian matrix and can be expressed as follows,

$$\dot{\boldsymbol{J}} = \begin{bmatrix} (\boldsymbol{w}_1 \times \boldsymbol{s}_1)^T & ((\boldsymbol{\omega}\times\boldsymbol{q}_1)\times\boldsymbol{s}_1 + \boldsymbol{q}_1 \times (\boldsymbol{w}_1 \times \boldsymbol{s}_1))^T \\ \vdots & \vdots \\ (\boldsymbol{w}_6 \times \boldsymbol{s}_6)^T & ((\boldsymbol{\omega}\times\boldsymbol{q}_6)\times\boldsymbol{s}_6 + \boldsymbol{q}_6 \times (\boldsymbol{w}_6 \times \boldsymbol{s}_6))^T \end{bmatrix}, \tag{3}$$

where $\boldsymbol{s}_i$ is the unit vector of every link; $\boldsymbol{w}_i$ the rotational angular velocity of every link; $\boldsymbol{\omega} = [\omega_x\ \omega_y\ \omega_z]^T$ the rotational angular velocity of the payload platform.

International Journal of Information, Control and Computer Sciences
ISSN: 2517-9942
Vol:3, No:12, 2009

So the joint space dynamic model can be expressed as follows,

$$\boldsymbol{M_l}(\boldsymbol{X})\ddot{\boldsymbol{L}} + \boldsymbol{H_l}(\boldsymbol{X},\dot{\boldsymbol{X}}) = \boldsymbol{F_l} + \boldsymbol{D_l}, \tag{4}$$

where $\boldsymbol{M_l}(\boldsymbol{X}) = \boldsymbol{J}^{-T}\boldsymbol{M}(\boldsymbol{X})\boldsymbol{J}^{-1}$,

$\boldsymbol{H_l}(\boldsymbol{X}) = \boldsymbol{J}^{-T}\boldsymbol{H}(\boldsymbol{X},\dot{\boldsymbol{X}}) - \boldsymbol{J}^{-T}\boldsymbol{M}(\boldsymbol{X})\boldsymbol{J}^{-1}\dot{\boldsymbol{J}}\dot{\boldsymbol{X}}$, $\boldsymbol{D_l}$ is the external disturbance transformed to joint space.

III. Fuzzy Disturbance Observer (FDO) Based Adaptive Controller

The classical control method for Stewart platform is the computed torque controller (CTC), which makes use of dynamic model information to compensate the highly nonlinearity of Stewart platform and proves to be effective. But in real world application, external disturbance is common and CTC completely ignores its influence. That will cause the degradation of controller's tracking performance and even make the whole system unstable.

For electro-mechanical system, external disturbance is generally compensated by two means: (a) High gain methods such as sliding control and etc. This kind of method can not avoid chattering effect and thus will cause the saturation of actuators. (b) Observer-based methods such as disturbance observer (DOB) [7] and etc. For the reason that DOB is based on linear system theory, it can not be applied in nonlinear system like Stewart platform. To overcome the defect of DOB, Kim [8] proposes a fuzzy disturbance observer (FDO) based on the theory that fuzzy system is a universal approximator [9]. The FOB can observe both external disturbance and internal model error. In this paper, we will incorporate CTC in joint space and FDO to construct the controller.

A. Controller Form

The standard nonlinear system equations can be derived as follows,

$$\dot{\boldsymbol{x}}_1 = \boldsymbol{x}_2$$

$$\dot{\boldsymbol{x}}_2 = -\boldsymbol{M}_l^{-1}\boldsymbol{H}_l + \boldsymbol{M}_l^{-1}\boldsymbol{u} + \boldsymbol{d} = -\boldsymbol{M}_l^{-1}\boldsymbol{H}_l + \boldsymbol{M}_l^{-1}\boldsymbol{u} + \boldsymbol{\Omega}, \tag{5}$$

where $\boldsymbol{x}_1 = \boldsymbol{L}$, $\boldsymbol{x}_2 = \dot{\boldsymbol{L}}$, $\boldsymbol{\Omega} = \boldsymbol{d}$ is the external disturbance. The effect of applying FOB is to approximate external disturbance $\boldsymbol{\Omega}$ with fuzzy system $\hat{\boldsymbol{\Omega}}$ and cancel external disturbance with feedforward method. The controller can be expressed as,

$$\boldsymbol{u} = \frac{\boldsymbol{v} + \boldsymbol{M}_l^{-1}\boldsymbol{H}_l - \hat{\boldsymbol{\Omega}}}{\boldsymbol{M}_l^{-1}}, \tag{6}$$

where $\boldsymbol{v}$ can be any feedback controller, in this paper we use CTC as $\boldsymbol{v}$ signal.

B. Velocity Observer (VO) Design

The position information of links can be obtained by photoelectric encoders integrated in joint torque motors. The velocity information of links can be measured by tachogenerator. But that will introduce severe noise information. Another method is differentiation of position information and then through a low-pass filter. Due to the delay effect of low-pass filter, the bandwidth of the controller will be lowered. In this paper, we will introduce a velocity observer [10] to obtain links' velocity information. Consider the following observer,

$$\dot{\hat{\boldsymbol{x}}}_1 = \hat{\boldsymbol{x}}_2 + \boldsymbol{G_D}\tilde{\boldsymbol{x}}_1,$$

$$\dot{\hat{\boldsymbol{x}}}_2 = \boldsymbol{M}_l^{-1}(-\boldsymbol{H}_l + \boldsymbol{u}) + \boldsymbol{G_P}\tilde{\boldsymbol{x}}_1 + \hat{\boldsymbol{\Omega}}, \tag{7}$$

where $\boldsymbol{G_D}, \boldsymbol{G_P}$ are gains of the observer. Define observation errors as follow,

$$\tilde{\boldsymbol{x}}_1 = \boldsymbol{x}_1 - \hat{\boldsymbol{x}}_1,$$

$$\tilde{\boldsymbol{x}}_2 = \boldsymbol{x}_2 - \hat{\boldsymbol{x}}_2. \tag{8}$$

Then the observation errors dynamic equations of velocity observer can be expressed as

$$\dot{\tilde{\boldsymbol{x}}}_1 = \tilde{\boldsymbol{x}}_2 - \boldsymbol{G_D}\tilde{\boldsymbol{x}}_1,$$

$$\dot{\tilde{\boldsymbol{x}}}_2 = (\boldsymbol{\Omega} - \hat{\boldsymbol{\Omega}}) - \boldsymbol{G_P}\tilde{\boldsymbol{x}}_1. \tag{9}$$

C. Fuzzy Disturbance Observer (FDO) Design

For the nonlinear system expressed in (5), the dynamic model of FDO can be expressed as follows,

$$\dot{\boldsymbol{\mu}} = -\sigma\boldsymbol{\mu} + \sigma\boldsymbol{x}_2 - \boldsymbol{M}_l^{-1}\boldsymbol{H}_l + \boldsymbol{M}_l^{-1}\boldsymbol{u} + \hat{\boldsymbol{\Omega}}, \tag{10}$$

where σ is positive definite. Due to unavailable of $\boldsymbol{x}_2$, we use $\hat{\boldsymbol{x}}_2$ instead and then,

$$\begin{aligned}\dot{\boldsymbol{\mu}} &= -\sigma\boldsymbol{\mu} + \sigma\hat{\boldsymbol{x}}_2 - \boldsymbol{M}_l^{-1}\boldsymbol{H}_l + \boldsymbol{M}_l^{-1}\boldsymbol{u} + \hat{\boldsymbol{\Omega}} \\ &= -\sigma\boldsymbol{\mu} + \sigma\boldsymbol{x}_2 - \sigma\tilde{\boldsymbol{x}}_2 - \boldsymbol{M}_l^{-1}\boldsymbol{H}_l + \boldsymbol{M}_l^{-1}\boldsymbol{u} + \hat{\boldsymbol{\Omega}}\end{aligned} \tag{11}$$

Define observation error of FDO as $\boldsymbol{\zeta} = \boldsymbol{x}_2 - \boldsymbol{\mu}$, and then we can obtain the observation error dynamic model of FDO by subtracting (11) from (5):

$$\dot{\boldsymbol{\zeta}} = -\sigma\boldsymbol{\zeta} + (\boldsymbol{\Omega} - \hat{\boldsymbol{\Omega}}) + \sigma\tilde{\boldsymbol{x}}_2. \tag{12}$$

D. Controller Synthesis

The controller adopts the structure of feedback + feedforward. The feedback part uses CTC and the feedforward part uses FDO. The control output can be expressed as,

$$\boldsymbol{u} = \boldsymbol{M}_l[\ddot{\boldsymbol{x}}_d - \boldsymbol{K_D}(\hat{\boldsymbol{x}}_2 - \dot{\boldsymbol{x}}_d) - \boldsymbol{K_P}(\boldsymbol{x}_1 - \boldsymbol{x}_d) - \hat{\boldsymbol{\Omega}}] + \boldsymbol{H}_l, \tag{13}$$

where $\boldsymbol{K_D}, \boldsymbol{K_P}$ are gains of the controller. The controller's structure is showed in the fig. 1:

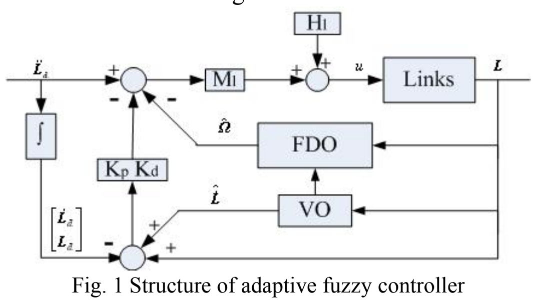

Fig. 1 Structure of adaptive fuzzy controller

Define tracking errors as $\boldsymbol{e}_1 = \boldsymbol{x}_1 - \boldsymbol{x}_d$, $\boldsymbol{e}_2 = \boldsymbol{x}_2 - \dot{\boldsymbol{x}}_d$, and put control output into Eq.5, we can get

$$\dot{\boldsymbol{e}}_1 = \boldsymbol{e}_2,$$

$$\dot{\boldsymbol{e}}_2 = -\boldsymbol{K_D}\boldsymbol{e}_2 - \boldsymbol{K_P}\boldsymbol{e}_1 + (\boldsymbol{\Omega} - \hat{\boldsymbol{\Omega}}) + \boldsymbol{K_D}\tilde{\boldsymbol{x}}_2. \tag{14}$$

Merge (9), (12) and (14) , and then we get

$$\dot{\boldsymbol{\Xi}} = \boldsymbol{\Pi\Xi} + \boldsymbol{B}(\boldsymbol{\Omega} - \hat{\boldsymbol{\Omega}}), \qquad (15)$$

where $\boldsymbol{\Xi} = [\tilde{\boldsymbol{x}}_1 \quad \tilde{\boldsymbol{x}}_2 \quad \boldsymbol{\zeta} \quad \boldsymbol{e}_1 \quad \boldsymbol{e}_2]^T$,

$$\boldsymbol{\Pi} = \begin{bmatrix} -\boldsymbol{G_D} & \boldsymbol{I} & 0 & 0 & 0 \\ -\boldsymbol{G_P} & 0 & 0 & 0 & 0 \\ 0 & \sigma\boldsymbol{I} & -\sigma\boldsymbol{I} & 0 & 0 \\ 0 & \boldsymbol{I} & 0 & 0 & 0 \\ 0 & \boldsymbol{K_D} & 0 & -\boldsymbol{K_P} & -\boldsymbol{K_D} \end{bmatrix},$$

$\boldsymbol{B} = [0 \quad \boldsymbol{I} \quad \boldsymbol{I} \quad 0 \quad \boldsymbol{I}]^T$.

Through proper choice of $\boldsymbol{G_P}$, $\boldsymbol{G_D}$, $\boldsymbol{K_P}$, $\boldsymbol{K_D}$ and σ, all eigenvalues of Π can ensure staying in the left side of complex plane. So there is symmetrical positive definite matrix $\boldsymbol{P}$ and make the following equation $\boldsymbol{\Pi}^T\boldsymbol{P} + \boldsymbol{P\Pi} = -\boldsymbol{Q}$ existed, where $\boldsymbol{Q}$ is a positive definite matrix. Define Lyapunov equation as

$$\mathrm{V} = \frac{1}{2}\boldsymbol{\Xi}^T\boldsymbol{P\Xi} + \frac{1}{2\gamma}\tilde{\boldsymbol{\theta}}^T\tilde{\boldsymbol{\theta}}, \qquad (16)$$

where γ is positive and $\hat{\theta}$ corresponds to learning speed. Choose $\dot{\hat{\boldsymbol{\theta}}} = \gamma\boldsymbol{\Xi}^T\boldsymbol{PB}\boldsymbol{\xi}^T$, we can prove that $\dot{\mathrm{V}}$ keeps negative outside a compact set, which ensures the tracking error and observation errors of VO and FDO are uniformly ultimately bounded (UUB) [11]. The specific proving process can be found in [8].

IV. Controller Modification Considering Actuator Saturation

Due to the randomness and non-prediction of external disturbance, the disturbance observer may be unstable if disturbance is large enough to reach the actuator's limit. In this situation, the observer can not observe the disturbance correctly and the performance of the whole system can not be ensured.

Eq(11) is dynamic model of practical system, can be expressed as,

$$\dot{\boldsymbol{x}}_2 = -\boldsymbol{M}_l^{-1}\boldsymbol{H}_l + \boldsymbol{M}_l^{-1}sat(\boldsymbol{u}) + \boldsymbol{\Omega}, \qquad (17)$$

where

$$sat(u) = \begin{cases} u_{\max}, & u > u_{\max} \\ u, & -u_{\max} \le u \le u_{\max} \\ -u_{\max}, & u < -u_{\max} \end{cases}$$

and $sat(\boldsymbol{u})$ corresponds to saturation operation for every element of vector $\boldsymbol{u}$, $u_{\max}$ is the maximal force every single actuator can afford. Then the Eq.12 can be modified to the following form,

$$\dot{\boldsymbol{\zeta}} = -\sigma\boldsymbol{\zeta} + (\boldsymbol{\Omega} - \hat{\boldsymbol{\Omega}}) + \boldsymbol{M}_l^{-1}(sat(\boldsymbol{u}) - \boldsymbol{u}) + \sigma\tilde{\boldsymbol{x}}_2. \qquad (18)$$

As soon as the actuator saturation appears, $\boldsymbol{M}_l^{-1}(sat(\boldsymbol{u}) - \boldsymbol{u})$ part will cause divergence of disturbance observer error.

In order to deal with the above divergence problem, we add saturation compensation operation into both FDO and VO, to ensure precisely observation of external disturbance and velocity signal under actuator saturation situation. The modified equations are as follows,

$$\dot{\boldsymbol{\mu}} = -\sigma\boldsymbol{\mu} + \sigma\hat{\boldsymbol{x}}_2 - \boldsymbol{M}_l^{-1}\boldsymbol{H}_l + \boldsymbol{M}_l^{-1}sat(\boldsymbol{u}) + \hat{\boldsymbol{\Omega}}, \qquad (19)$$

$$\dot{\hat{\boldsymbol{x}}}_2 = \boldsymbol{M}_l^{-1}(-\boldsymbol{H}_l + sat(\boldsymbol{u})) + \boldsymbol{G_P}\tilde{\boldsymbol{x}}_1 + \hat{\boldsymbol{\Omega}}. \qquad (20)$$

V. Real-time Trajectory Shaping under Actuator Saturation

When the reference trajectory changes too rapidly, there is necessity to modify the reference acceleration to keep the controller operate within the non-saturated state. The main idea is making use of dynamic model information to limit the maximal actuator force in joint space and then computing the modified reference acceleration in operational space.

The operational space dynamic model of Stewart platform can be transformed as follows,

$$\ddot{\boldsymbol{Z}} = \boldsymbol{T} \cdot \boldsymbol{F} = [\boldsymbol{t}_1, \boldsymbol{t}_2, \boldsymbol{t}_3, \boldsymbol{t}_4, \boldsymbol{t}_5, \boldsymbol{t}_6] \cdot \boldsymbol{F}, \qquad (21)$$

where $\ddot{\boldsymbol{Z}} = \ddot{\boldsymbol{X}} + \boldsymbol{H}(\boldsymbol{X}, \dot{\boldsymbol{X}}) / \boldsymbol{M}(\boldsymbol{X}) = [\ddot{z}_1, \ddot{z}_2, \ddot{z}_3, \ddot{z}_4, \ddot{z}_5, \ddot{z}_6]^T$ is introduced to simply the dynamic equation. $\boldsymbol{T} = \boldsymbol{J}^T / \boldsymbol{M}(\boldsymbol{X})$ is the projection matrix, $\boldsymbol{t}_i$ is the i th column vector of $\boldsymbol{T}$.

From (21), we can see that there is a transformation between actuator force and payload platform acceleration. Due to the limited force output capability of actuators, payload platform acceleration has a boundary which is changing with manipulator dynamics. If the acceleration of the reference trajectory is beyond that boundary, actuator saturation will happen. So the function of the trajectory shaping algorithm is to modify the reference trajectory acceleration and move it into the maximum acceleration boundary, assuming that the modification's influence to dynamic performance of Stewart platform is as small as possible. The maximum acceleration boundary can be expressed as follows,

$$\Omega(\ddot{\boldsymbol{Z}}) = \left\{ \ddot{\boldsymbol{Z}} = \sum_{i=1}^{6} \boldsymbol{t}_i f_i \,\middle|\, f_i \in \Omega^F \right\}, \qquad (22)$$

where f_i is the i th the column vector of $\boldsymbol{F}$, Ω^F is the boundary of actuator's output force, $\Omega(\ddot{\mathrm{Z}})$ is the maximum acceleration boundary of Stewart platform. We illustrate the mapping of acceleration boundary by a 2D case (fig.2) for Eq.(22) is 6D and hard to explain.

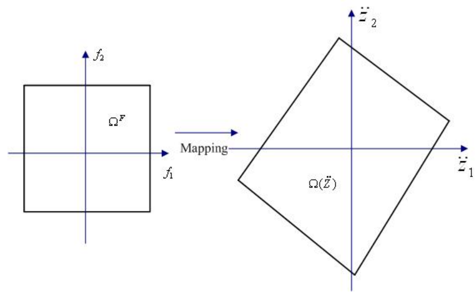

Fig. 2 The acceleration modification in 2D situation

Because actuator saturation is with f_i, we choose $\{\boldsymbol{t}_1, \boldsymbol{t}_2, \boldsymbol{t}_3, \boldsymbol{t}_4, \boldsymbol{t}_5, \boldsymbol{t}_6\}$ as basis. The reference value of $\ddot{\boldsymbol{Z}}$

can be expressed as a linear combination of basis elements

$$\ddot{\boldsymbol{Z}}^{ref} = \sum_{i=1}^{6} \boldsymbol{t}_i \lambda_i \,,\; \lambda_i \in \Omega^F \tag{23}$$

where λ_i can be obtain by projecting $\ddot{\boldsymbol{Z}}^{ref}$ on the basis $\{\boldsymbol{t_1}, \boldsymbol{t_2}, \boldsymbol{t_3}, \boldsymbol{t_4}, \boldsymbol{t_5}, \boldsymbol{t_6}\}$:

$$\lambda_i = \frac{\boldsymbol{t}_i^T \cdot \ddot{\boldsymbol{Z}}^{ref}}{\boldsymbol{t}_i^T \cdot \boldsymbol{t_i}} \,. \tag{24}$$

If λ_i is not within Ω^F, we modify $\ddot{\boldsymbol{Z}}^{ref}$ and make it stay in the boundary

$$\ddot{\boldsymbol{Z}}^{\boldsymbol{mod}} = \sum_{i=1}^{6} \boldsymbol{t_i} \lambda_i \gamma_i \,,\; \gamma_i = \begin{cases} 1.0, & \lambda_i \in \Omega^F \\ \left|\dfrac{f_i^{\max}}{\lambda_i}\right|, & \lambda_i \notin \Omega^F \end{cases} . \tag{25}$$

where $f_i^{\max}$ is the maximum force of the i th link. Here $f_i^{\max}$ is not equal to $u_{\max}$, which is the maximum output force of the actuator. Considering the external disturbance, $f_i^{\max}$ can be expressed as $f_i^{\max} = u_{\max} - \hat{\Omega}_i$, where $\hat{\Omega}_i$ is the i th element of $\hat{\boldsymbol{\Omega}}$. The modified acceleration trajectory is $\ddot{\boldsymbol{X}}^{\boldsymbol{mod}} = \ddot{\boldsymbol{Z}}^{\boldsymbol{mod}} - \boldsymbol{H}(\boldsymbol{X}^{ref}, \dot{\boldsymbol{X}}^{ref}) / \boldsymbol{M}(\boldsymbol{X}^{ref})$. Where $\boldsymbol{X}^{ref}$ and $\dot{\boldsymbol{X}}^{ref}$ are reference position and velocity of Stewart platform. The trajectory shaping algorithm can be demonstrated with a 2D case again as fig.3.

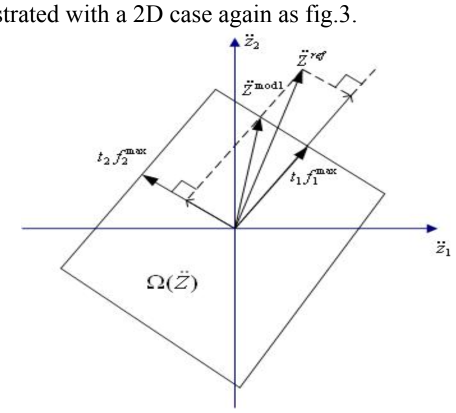

Fig. 3 The acceleration modification in 2D situation

Although the above trajectory shaping algorithm solves the problem of actuator saturation, it also introduces the position error of the reference trajectory. So we need a further modification for the acceleration of reference trajectory as soon as the actuators are back to non-saturated state. It will force position error of the reference trajectory converge to zero. The modification can be expressed as follows,

$$\ddot{\boldsymbol{X}}^{\boldsymbol{mod}} = \ddot{\boldsymbol{X}}_{ref} + A_d(\dot{\boldsymbol{X}}^{ref} - \dot{\boldsymbol{X}}^{\mathrm{mod}}) + A_p(\boldsymbol{X}^{ref} - \boldsymbol{X}^{\mathrm{mod}}) \,, \tag{26}$$

where A_p and A_d are gain for the modification.

VI. Computer Simulation

In this section, the proposed adaptive fuzzy controller and trajectory shaping scheme under actuator saturation will be evaluated. The dynamic model and its parameters used in computer simulation is based on a Stewart platform in our laboratory. The weight of payload platform is $45.2kg$. The center of gravity is $[0 \quad 0 \quad 0.25]m$. The inertial moment is $diag([12.7 \quad 14.6 \quad 13.1])kg \cdot m^2$. The saturation force of the actuators is 2000N. And the parameters of the controller are chosen as: $\boldsymbol{K_D}$ is $100\boldsymbol{E_6}$; $\boldsymbol{K}_P$ is $1000\boldsymbol{E_6}$; $\boldsymbol{G_D}$ is $10\boldsymbol{E_6}$; $\boldsymbol{G_P}$ is $100\boldsymbol{E_6}$; σ is 100 ; γ is 1000 , where $\boldsymbol{E}_6$ is the 6×6 identity matrix.

The simulation will compare three kinds of control schemes: conventional computed torque controller (CTC), computed torque controller with real-time trajectory shaping (CTCRTS) and FDO based adaptive controller with real-time trajectory shaping (FDORTS). The reference trajectory used in simulation is the sine wave applied both in X axis and Y axis. The period of the sine wave is 1s and the amplitude is 0.5m. Furthermore, an external disturbance of 100N is exerted on the first link of the Stewart platform at the end of 1s. The simulation results are shown in following figures.

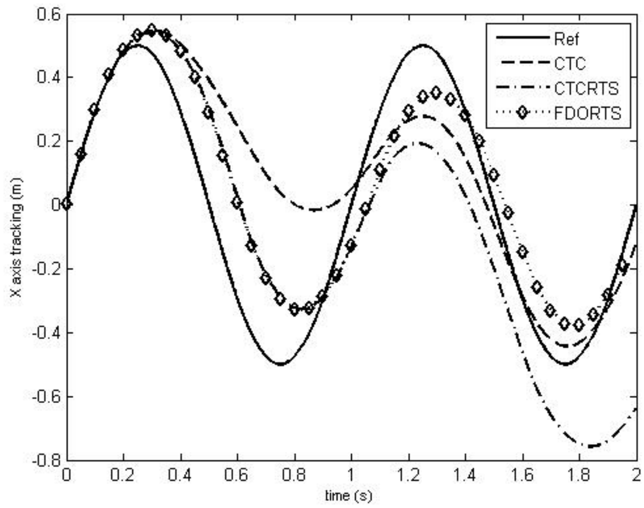

Fig. 4 Comparison of X axis tracking

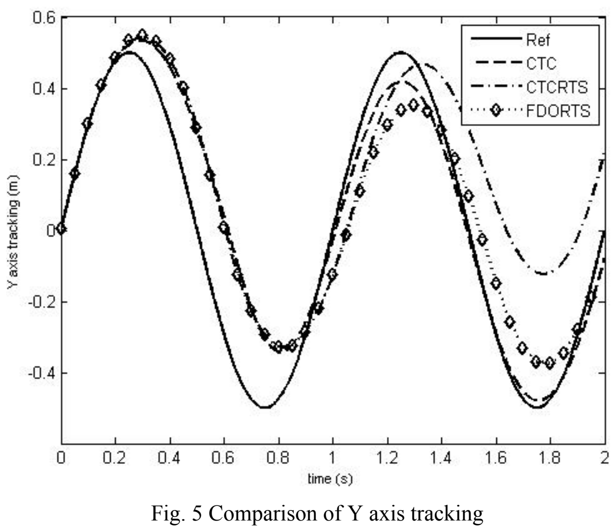

Fig. 5 Comparison of Y axis tracking

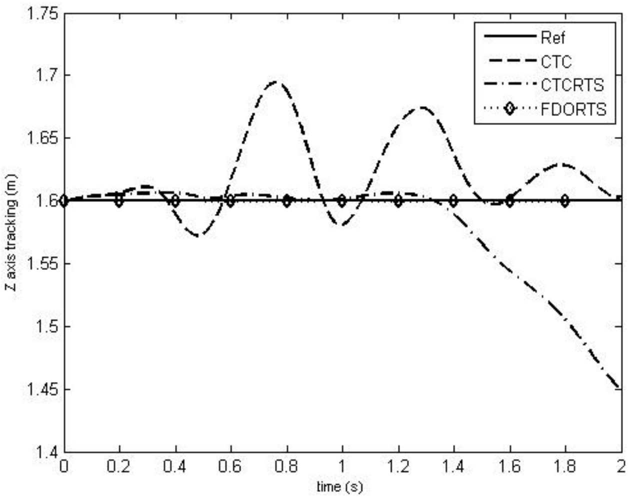

Fig. 6 Comparison of Z axis tracking

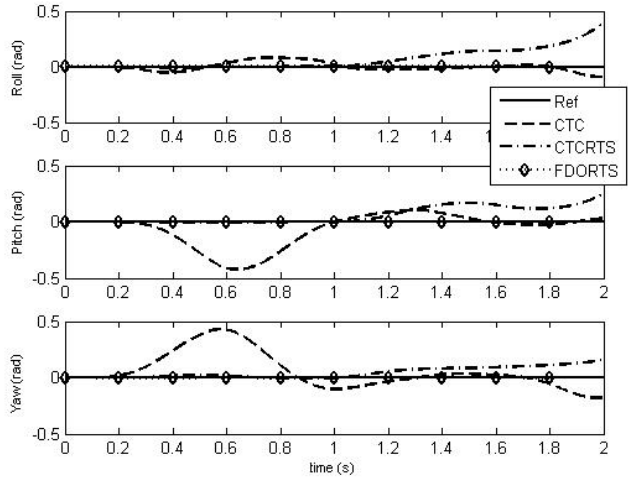

Fig. 7 Comparison of rotational axis tracking

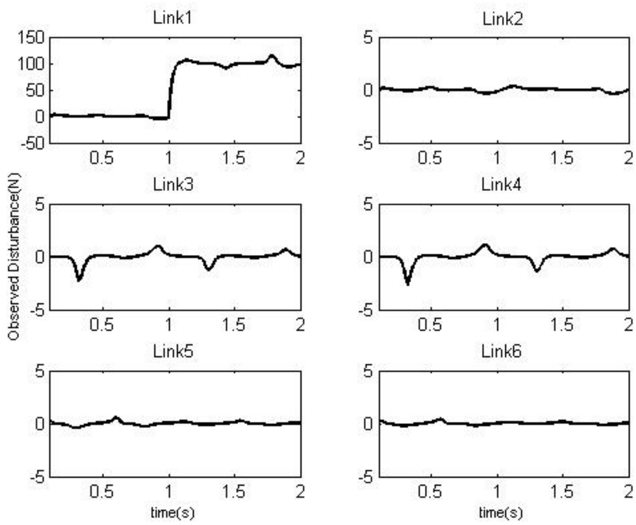

Fig. 8 Disturbance Observing Results on Different Links

As we can see from the above figures, due to actuator saturation, CTC performs bad and produces undesirable motion. If the reference trajectory varies severely, the controller may even turn to unstable. CTCRTS performs better than CTC during simulation time of 0~1s thanks to its inclusion of real-time trajectory shaping algorithm. Actuator saturation situation does not happen and no undesirable coupling motion is observed. But during simulation time of 1~2s, CTCRTS produces large tracking error and finally becomes divergence under the influence of external disturbance. By contrast, FDORTS can precisely estimate the external disturbance and cancel it. Both stability and tracking performance are ensured for the Stewart platform with the proposed control scheme.

VII. Conclusion

We propose an adaptive fuzzy controller and real-time trajectory shaping scheme for Stewart platform under actuator saturation in this paper. The real-time trajectory shaping algorithm makes use of dynamic model information to predict saturation condition and thus modifies the reference trajectory. The adaptive fuzzy controller combines computing torque controller, link velocity observer and fuzzy disturbance observer with the saturation compensation. It can ensure stability and tracking performances of the controller in present of external disturbance and position only measurement. Further is required verification of the performances of the control scheme in a practical Stewart platform by means of algorithm.

References

[1] J. P. Merlet, Parallel Robots (2nd), Berlin: Springer, 2006.

[2] D. Bernstein and A. Michel, “A chronological bibliography on saturating actuators” International Journal of Robust and Nonlinear Control, vol. 5, no.5, pp. 375-380, 1995.

[3] E. N. Johnson and A. J. Calise, “Neural network adaptive control of systems with input saturation”, Proceedings of IEEE American Control Conference, pp. 3527-3532, 2001.

[4] K. Ohishi, K. Akahori, W. Kaewprom and et al, “Robust manipulator control method considering limit values of torque and controller output”, Proceedings of the IEEE IECON 22nd International Conference, pp. 1252-1257, 1996.

[5] M. V. Kothare, P. J. Campo, M. Morari and et al, “A unified framework for the study of anti-windup designs” Automatica, vol. 30, no. 12, pp.1869-1883, 1994.

[6] Y. I. Lee and B. Kouvaritakis, “Receding horizon output feedback control for linear systems with input saturation” Proceedings of the 39th IEEE Conference on Decision and Control, pp. 656-661, 2000.

[7] K. Ohnishi, “A new servo method in mechatronics” Trans. Japanese Society of Electrical Engineering, vol. 107-D, pp. 83-6, 1987.

[8] E. Kim, “A fuzzy disturbance observer and its application to control” IEEE Trans. on Fuzzy Systems, vol. 10, no. 1, pp. 77-82, 2002.

[9] L. X. Wang and J. M. Mendel, “Fuzzy basis functions, universal approximation, and orthogonal least-squares learning” IEEE Trans. on Neural Networks, vol. 3, no. 5, pp. 807-814, 1992.

[10] S. Nicosia and P. Tomei, “Robot control by using only joint position measurements” IEEE Trans on Automatic Control, vol. 35, no. 9, pp. 1058-1061, 1990.

[11] M. J. Corless and G. Leitmann, “Continuous state feedback guaranteeing uniform ultimate boundedness for uncertain dynamic systems” IEEE Trans on Automatic Control, vol. AC-26, no. 5, pp. 1139-1144, 1981.